Solar Phys (2007) 241: 351–370
DOI 10.1007/s11207-007-0277-8

Circular Polarization Observed in Interplanetary Type III Radio Storms

M.J. Reiner · J. Fainberg · M.L. Kaiser · J.-L. Bougeret

Received: 24 July 2006 / Accepted: 1 February 2007 /
Published online: 23 March 2007

Abstract We report the detection and analysis of circular polarization in solar type III radio storms at hectometric-to-kilometric wavelengths. We find that a small (usually less than 5%), but statistically significant, degree of circular polarization is present in all interplanetary type III radio storms below 1 MHz. The sense of the polarization, which is right-hand circular for some storms and left-hand circular for others, is maintained for the entire duration of the type III storm (usually many days). For a given storm, the degree of circular polarization peaks near central meridian crossing of the associated active region. At a given time, the degree of circular polarization is found to generally vary as the logarithm of the observing frequency. The radiation characteristics, including the polarization, for one interplanetary type III storm exhibits an unusual 1.6 hour oscillation. Based on the standard plasma emission theory of type III radiation, we discuss the implications of these observations for the magnitude and radial dependence of the solar magnetic field above active regions on the Sun.

1. Introduction

Radio emissions from the Sun at hectometric-to-kilometric wavelengths consist mainly of type II (Malitson, Fainberg, and Stone, 1973; Cane *et al.*, 1982) and type III (Hartz, 1969; Fainberg and Stone, 1974) radio bursts. In the last two decades, various aspects of individual type III bursts have been extensively studied: radiation modes, radiation propagation and scattering, exciter speeds, interplanetary trajectories, low-frequency limits, finite source

M.J. Reiner (✉)
The Catholic University of America and NASA/Goddard Space Flight Center, Code 674,
Greenbelt, Maryland, USA
e-mail: michael.reiner@gsfc.nasa.gov

J. Fainberg · M.L. Kaiser
NASA/Goddard Space Flight Center, Greenbelt, Maryland, USA

J.-L. Bougeret
Observatoire de Paris, Meudon, France

modeling, *etc.* (Kellogg, 1980; Steinberg *et al.*, 1984; Steinberg, Hoang, and Dulk, 1985; Dulk, Steinberg, and Hoang, 1984; Dulk *et al.*, 1985, 1987, 1998; Kellogg, 1986; Reiner and Stone, 1986, 1989, 1990; Lecacheux *et al.*, 1989; Reiner, Stone, and Fainberg, 1992; Reiner, Fainberg, and Stone, 1995; Leblanc *et al.*, 1996; Reiner *et al.*, 1998; Reiner and Kaiser, 1999; Reiner, 2001). Type III radiation is generated by the well-established plasma emission mechanism (Ginzburg and Zheleznyakov, 1958), implying that the remotely observed radiation is produced at the fundamental and harmonic of the plasma frequency in the radio source region (also see Robinson, 1992; Robinson, Cairns, and Gurnett, 1993).

Type III storms are semi-continuous emissions consisting of thousands of weak type III bursts per day. These radio emissions are produced by low-energy electrons ($\approx$2 keV) that are injected from quasi-stable active regions on the Sun and propagate along the magnetic field lines through interplanetary space (Potter, Lin, and Anderson, 1980). Type III radio storms are known to be associated with metric type I noise storms, which in turn are associated with solar active regions (Boishot, De la Noë, and Møller-Pedersen, 1970; Sakurai, 1971; Stewart and Labrum, 1972; Kayser *et al.*, 1987).

Type III radio storms at hectometric-to-kilometric wavelengths, first detected by radio receivers on the Radio Astronomy Explorer (RAE-1) spacecraft, were utilized to derive the electron plasma density profile along the path of the electron beam through the interplanetary medium, to determine the solar wind speed, and to determine the electron exciter speeds (Fainberg and Stone, 1970a, 1970b, 1971). Subsequently, the radio source direction-finding capabilities on the International Sun – Earth Explorer (ISEE-3) (renamed International Cometary Explorer (ICE)) spacecraft were used to determine the locations of the centroids of the type III storm sources at decreasing frequencies, corresponding to increasing distances from the Sun, to deduce the spatial path of the underlying electron beam (Bougeret, Fainberg, and Stone, 1983, 1984a, 1984b). These latter results confirmed that the electron beam follows an Archimedean spiral path through interplanetary space (Parker, 1958). The direction-finding results on ISEE-3 were also used to confirm that the interplanetary (kilometric) storms originated near solar active regions and their associated type I noise storms (Kayser *et al.*, 1987). Type III radio storms were also found to generally cease, or at least greatly diminish in intensity, at the time of major coronal eruptions at the associated active region (Reiner *et al.*, 2001).

Metric type III storms, observed at high frequencies ($>$20 MHz) by ground-based observatories, exhibit circular polarization (up to about 25%) (Kai, Melrose, and Suzuki, 1985). In this paper, we report on the circular polarization of type III radio storms below 1 MHz. We find that there is a small, but statistically significant, degree of circular polarization in all interplanetary type III storms. The sense of the polarization, for a given storm, can be either right-hand or left-hand circular, and this polarization sense is maintained for the entire period of observation of a given storm. Furthermore, we find that the degree of circular polarization for a given storm peaks near central meridian crossing of the corresponding radio sources and decreases systematically with decreasing frequency. Finally, assuming that the measured degree of circular polarization is proportional to the ratio of the electron cyclotron frequency to the plasma frequency, as implied by the theory of type III emissions, we use these remote observations of the wave polarization to deduce information on the strength and radial behavior of the magnetic fields above solar active regions.

2. Instrument Description

The radio observations discussed here were provided by the WAVES radio instrument on the *Wind* spacecraft. This instrument includes several radio receivers that cover the frequency

range from 4.0876 kHz to 13.825 MHz (Bougeret *et al.*, 1995). The radio receivers used in the present analysis were the superheterodyne (step-tuned) receivers (RAD1), which cover the frequency range from 20 to 1040 kHz at 32 discrete frequencies (selected from 256 frequency channels) with a highest sampling rate of 45.8 seconds and a bandwidth of 3 kHz. These receivers are connected to a dipole antenna (50 meter elements) in the spacecraft spin plane and a dipole antenna (5.28 meter elements) along the spacecraft spin axis.

The radio receivers on *Wind* were specifically designed to permit both the full 2-D direction-finding and polarization analysis of an incident wave. This is done by combining signals from the spin-plane and spin axis antennas to form synthesized signals of the incoming wave electric vectors (Manning and Fainberg, 1980). It was shown there that the analysis of the synthesized signal patterns that result from the 3-second spacecraft spin period permits the determination of the four Stokes parameters (S, V, U, Q) (Kraus, 1986), in addition to the two angles describing the line-of-sight direction to the radio source and the angular radius of the source, assuming that the source can be represented by a circular disk of uniform brightness.

3. Analysis of the Spatial and Radiation Characteristics of Interplanetary Type III Storms

The *Wind* spacecraft was launched, near solar minimum, in November of 1994. The first weak interplanetary type III radio storm was observed about a month later, beginning on 18 December 1994 and lasting for about two days. During 1995, weak type III storms were observed starting on 3 March, 28 March, and 16 October. Analysis of these latter storms indicated that the radiation from each was weakly circular polarization. The next type III storm was not observed until 8 months later, on 10 July 1996. Only two type III storms were observed during 1996, the other one beginning on 24 November. As solar maximum approached, the occurrence rate of type III storms progressively increased. Near solar maximum in 2000 – 2001, WAVES detected, on average, one or two type III storms per month (Kaiser, 2003).

In addition to the spatial characteristics of the radio sources associated with the interplanetary type III storms established from previous spacecraft missions, the analysis of the type III storm radiation observed by the WAVES instrument on the *Wind* spacecraft indicates unequivocally that the type III storm radiation, observed during solar cycle 23, is weakly polarized below 1 MHz. Furthermore, since the semi-continuous radiation from a given type III storm remains at a nearly constant level for at least several days, the resulting large statistical sample enables us to accurately quantify the degree of circular polarization and establish its variation with observing frequency and with time. In this section we illustrate the spatial and radiation characteristics of interplanetary type III storms with two representative examples. We also present the analysis of two other storms that are rare and rather unusual: one that had an unusually high degree of circular polarization and another that exhibited 1.6-hour oscillations in several of the measured source parameters.

3.1. Interplanetary Type III Storm in June of 2004

A radio dynamic spectrum showing the type III storm on 20 June 2004 is provided in Figure 1. The frequency range is from 20 to 1040 kHz. Typical of type III storms, this spectrum consists of thousands of weak, individual type III radio bursts during this 24 hour time period. Due to the relatively slow sweep time of the RAD1 receiver, it is not possible to resolve

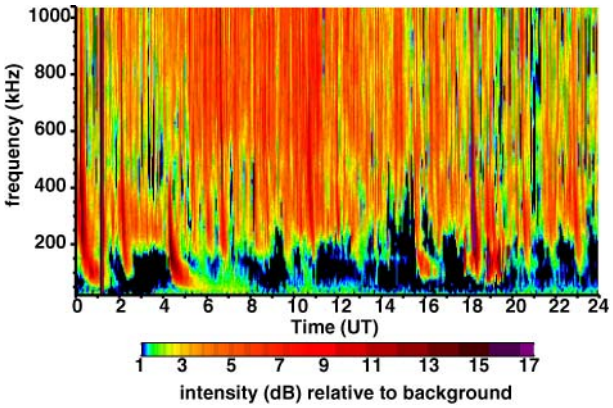

Figure 1 Dynamic spectrum of the *Wind*/WAVES radio data from 0 to 24 UT on 20 June 2004, The frequency range (vertical axis) is from 20 to 1040 kHz.

each of the individual type III bursts. These storm bursts have a typical low-frequency limit of about 150 kHz, but generally extend well above 1 MHz (Stewart and Labrum, 1972). Specifically, for this interplanetary type III storm, metric storm emissions were observed to frequencies of about 60 MHz by the Green Bank Solar Radio Burst Spectrometer (GBSRB) from 18 to 21 June (http://www.astro.umd.edu/~white/gb/).

This type III storm was first observed on about 14 June when two likely associated active regions, NOAA 10634 and 10635, appeared at the east limb of the Sun, the first to the north, and the second to the south of the solar equator. During this period, the Nançay radioheliograph observed a type I noise storm, associated with NOAA 10635, in the southern hemisphere, so this active region is the likely origin of the interplanetary type III storm. These interplanetary storm emissions were observed continuously for 11 days, until 25 June 2004, by which time the associated active region had corotated to near the west limb of the Sun.

The results of the direction-finding and polarization analysis on 20 June 2004 at the highest RAD1 frequency of 1040 kHz, are displayed in Figure 2. The radio source parameters were deduced from the best simultaneous fit to three independent antenna responses. The output parameters are the source flux density, azimuth, colatitude, angular radius, and circular polarization.

In obtaining the results shown in Figure 2, we subtracted the galactic background before performing the despin analysis. Specifically, we first determined the modulation pattern of the very stable galactic background component during a particularly quiet time period on 9 June 2004, when there was no evidence of any radiation other than the galactic background. The modulation pattern of the galactic background component, which was deduced by averaging the galactic signal over many spacecraft spins, indicated a source azimuth of 80°, a colatitude of 110°, and a source angular radius of 70°. The derived Stokes parameter, $V = -0.000012 \pm 0.0013$, is consistent with zero, *i.e.*, no circular polarization.

This modulated galactic background signal, with azimuth of the galactic source projected to 20 June, was then subtracted, with proper phase, from the total modulated pattern observed during the time period of the type III storm. The resulting residual modulated signal from the storm emissions was then fit to the equations for the antenna response, yielding the physical parameters of the storm source, shown in Figure 2.

Figure 2a shows the demodulated source flux density in solar flux units (sfu) (1 sfu = 10^{-22} W m^{-2} Hz^{-1}). The observed burstiness in the flux density corresponds to the innumerable individual weak type III bursts. The flux density of type III storm at this time averaged

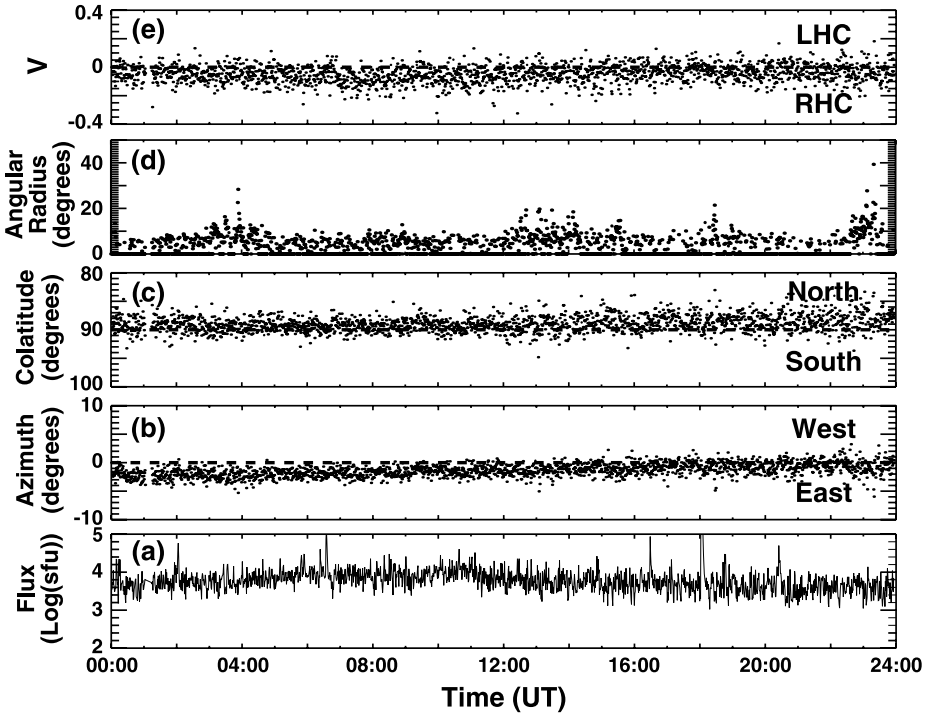

Figure 2 Results of the direction-finding/polarization analysis at 1040 kHz from 0 to 24 UT on 20 June 2004. (a) Radio source flux density as a function of time. (b) Radio source azimuth, relative to the *Wind* – Sun line. (c) Radio source colatitude, relative to the direction of the ecliptic plane. (d) Source angular radius. (e) Degree of circular polarization.

about $10^{3.8}$ sfu, which is about 8 dB above the level of the galactic background radiation ($10^{3.0}$ sfu).

Figures 2b and c show the results for the source directions deduced from this analysis. These are the line-of-sight directions to the radio source as determined by the spinning *Wind* spacecraft. Figure 2b presents the radio source azimuthal direction, relative to the spacecraft – Sun direction (0°): a negative angle corresponds to a source to the east of the *Wind* – Sun line; a positive angle, to the west of the *Wind* – Sun line. The derived azimuth for this radio source exhibits the east – west drift with time that is characteristic of type III radio storms. It drifts from about 2.5° to the east of the *Wind* – Sun line to near central meridian by the end of the day, reflecting the corotation of the radio source with the Sun during this time period.

Figure 2c presents the radio source colatitude, measured relative to the spacecraft spin plane (in the case of *Wind*, the ecliptic plane) for the same time period. Values less than (greater than) 90° correspond to the radio source lying to the north (south) of the ecliptic plane. Figure 2d presents the source angular radius deduced from the depth of the observed modulation pattern. The angular radius of the storm source at this frequency was about 5°, consistent with previous results from ISEE-3 storm observations (Bougeret, Fainberg, and Stone, 1984b).

The derived Stokes parameter V, which indicates the degree of circular polarization, is shown in Figure 2e. A value of 1 (-1) corresponds to 100% left (right)-hand circular

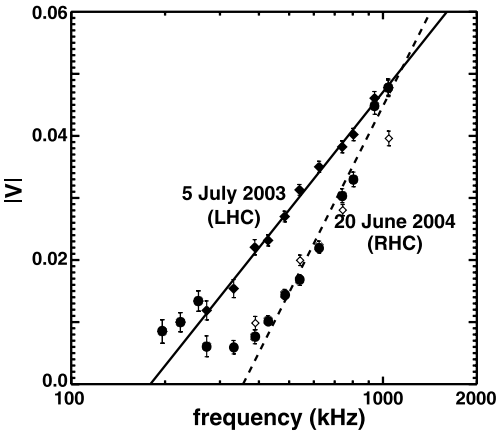

Figure 3 Mean values of the Stokes parameter $|V|$ as a function of observing frequency, deduced from the results of the direction-finding/polarization analysis for type III radio storms observed from 0 to 24 UT on 20 June 2004 (dots), on 5 July 2003 (solid diamonds), and on 2 July 2003 (open diamonds). The error bars correspond to the error in the mean. The sense of the polarization for each storm is also indicated. The straight lines represent the best fit to the higher frequency polarization values.

polarization. (Throughout this paper we use the convention that left-hand circular (LHC) polarization corresponds to the electric-field vector rotating clockwise with the wave approaching the observer (Kraus, 1986).) The derived values for V clearly indicate that during this period there was a small degree of right-hand circular (RHC) polarization. Averaging these data over the entire 24-hour time period gives a mean circular polarization of $V = -0.0478 \pm 0.0014$, *i.e.*, nearly 5% RHC. Since the underlying galactic component shows no evident circular polarization, this small degree of right-hand circular polarization must originate from the storm source.

Similar results for the type III radio storm source parameters were derived at other frequencies. The degree of circular polarization, averaged over the 24-hour period on 20 June, was found to decrease systematically with decreasing frequency. Figure 3 shows the mean values of $|V|$ determined at frequencies from 196 to 1040 kHz. On the semi-log plot these data are approximately linear, at least at the higher frequencies. At the lower frequencies (<400 kHz), the results may be affected by possible contamination from the highly polarized AKR radiation from Earth (Gurnett, 1975) and/or by possible plasma affects in the vicinity of the spacecraft. The straight-line fit (dashed line) to the higher frequency (>425 kHz) points corresponds to $|V| = -0.255 + 0.0433 \ln(f)$, where f is the observing frequency in kHz.

3.2. Interplanetary Type III Storm in July of 2003

Figure 4 shows a dynamic spectrum of the radio emissions for the 11 day period from 27 June through 7 July 2003. Type III storm activity was observed throughout this period. While there was some low-level storm-like emissions as early as 27 June (DOY = 178), significant storm activity did not begin until about the middle of 30 June (DOY = 181). At about this time the complex active region, NOAA 10397, in the northern solar hemisphere, appeared on the east limb of the Sun. Its association with a Nançay noise storm makes it the logical candidate as the solar origin of these type III storm emissions.

The corresponding derived source parameters are presented in Figure 5 for the 8 day period from 30 June through 7 July 2003. For greater clarity, we have plotted only every 16th data point. For this storm, we subtracted the modulated signal from the galactic component determined for a quiet period on 12 July.

Over this 8 day period, the storm flux, shown in Figure 5a, rose to a maximum of about $10^{3.9}$ sfu (9 dB above the galactic background) on 4 – 5 July (DOY = 185 – 186), as the

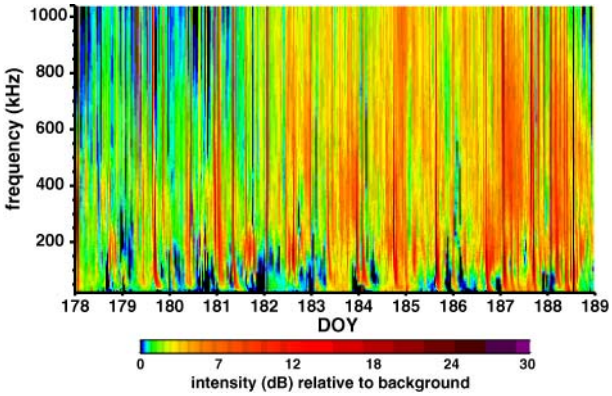

Figure 4 Dynamic spectrum of the *Wind*/WAVES radio data from 0 to 24 UT on 27 June through 7 July 2003. The frequency range (vertical axis) is from 20 to 1040 kHz.

associated active region complex crossed central meridian. It then decreased again as the active region approached the western limb. This is the typical long-term behavior of the radiation from interplanetary type III radio storms, and is likely the result of beaming of the type III radiation (Wright, 1980). Correspondingly, the source azimuth, shown in Figure 5b, drifted from about 5° to the east of the *Wind* – Sun line to about 5° west, after crossing central meridian late on 4 July, about half a day after NOAA 10397 crossed central meridian. Figure 5c indicates that the radio source was a few degrees to the north of the ecliptic plane, consistent with the northern hemisphere active region and the heliographic latitude of *Wind* of 3.2°. The derived angular radius of the source, shown in Figure 5d, was again about 5°.

Figure 5e shows that the radio source for this storm was weakly circularly polarized in the left-hand sense. The average degree of circular polarization on 5 July was found to be $V = +0.0478 \pm 0.0012$, indicating a statistically significant degree of circular polarization of about 5% LHC. The degree of circular polarization also exhibited a center-to-limb variation; it was near zero when the source was near the solar limbs and maximum when the source neared central meridian. This center-to-limb variation in the circular polarization is illustrated in greater detail in Figure 6a, which plots a running average of the measured circular polarization as a function of time over this 8 day period. The dashed curve in Figure 6a corresponds to $V = 0.044 \cos \beta$, where β is the solar longitude corresponding to a corotation rate of 13.3° per day. The measured degree of circular polarization qualitatively follows this curve, indicating that the variation in the circular polarization over this time period likely resulted from the different viewing angles of the radio source relative to the observer (see discussion below).

The intensity of this storm at central meridian crossing was similar to that of the June 2004 storm, but the radiation from these two storms was polarized in the opposite sense. As for the June 2004 storm, the degree of circular polarization measured for this July 2003 storm systematically decreased with decreasing frequency. Figure 3 also shows the mean values of V at measured frequencies from 196 to 1040 kHz, averaged over the 24-hour period on 5 July. Again, there is a clear linear relationship, but in this case the fall off is less steep. The best fit straight (solid) line, to the frequency data above 250 kHz, corresponds to $|V| = -0.142 + 0.0274 \ln(f)$, indicating that although the degree of circular polarization for these two storms are essentially the same at 1040 kHz, the frequency dependence is rather different. The open diamonds on Figure 3 show the circular polarization measured on 2 July 2003. We see that although the overall degree of polarization is systematically lower, the rate of fall off is essentially the same as on 5 July (see Discussion).

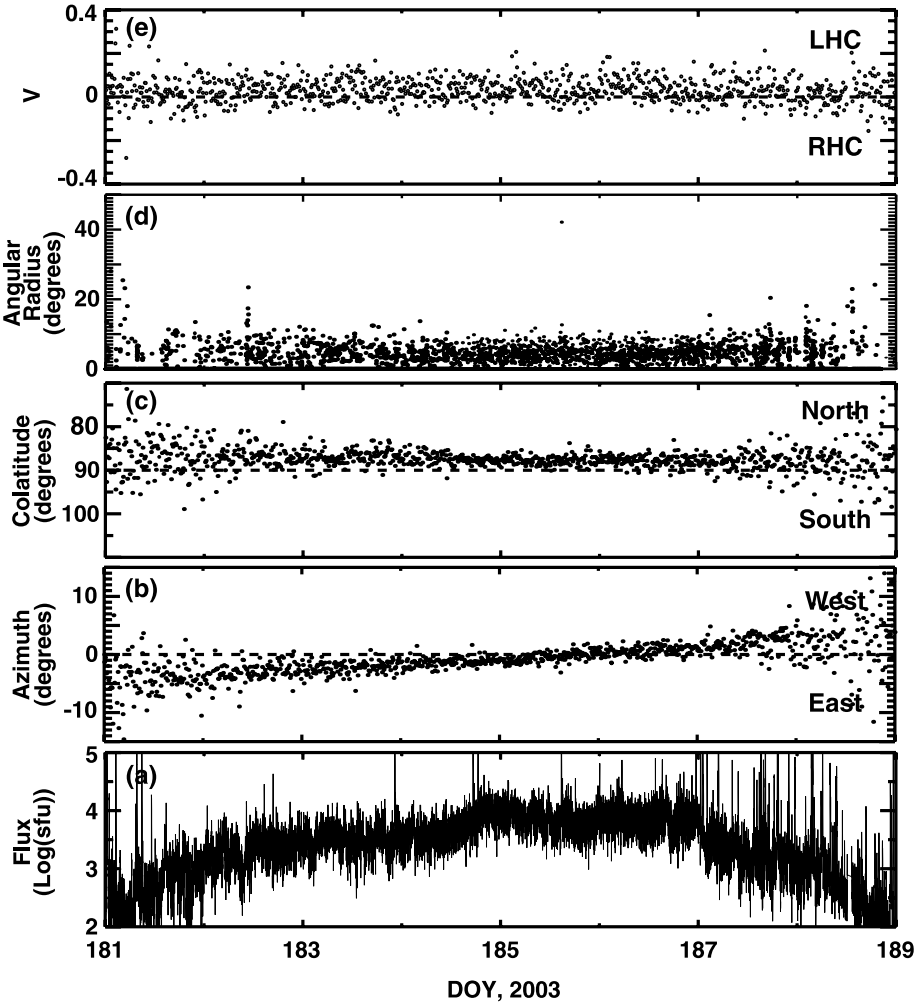

Figure 5 Results of the direction-finding/polarization analysis at 1040 kHz from 30 June through 7 July 2003. (a) Radio source flux density as a function of time. (b) Radio source azimuth, relative to the *Wind* – Sun line. (c) Radio source colatitude, relative to the direction of the ecliptic plane. (d) Source angular radius. (e) Degree of circular polarization.

3.3. Interplanetary Type III Storm in September of 2004

This type III radio storm commenced on 3 September and lasted until about 10 September 2004. It was likely associated with the active region complex, NOAA 10667 and 10669, both of which were in the southern solar hemisphere. A corresponding type I noise storm was observed by the Nançay radioheliograph in the southern hemisphere.

The radio source parameters on 8 September 2004, derived by subtracting the galactic component on 15 September, are shown in Figure 7. The lower panel shows that the flux density of this storm was similar to that of the previous storms; the average flux density at 1040 kHz was about $10^{3.9}$ sfu or 9 dB above the level of the galactic background. Figures 7b

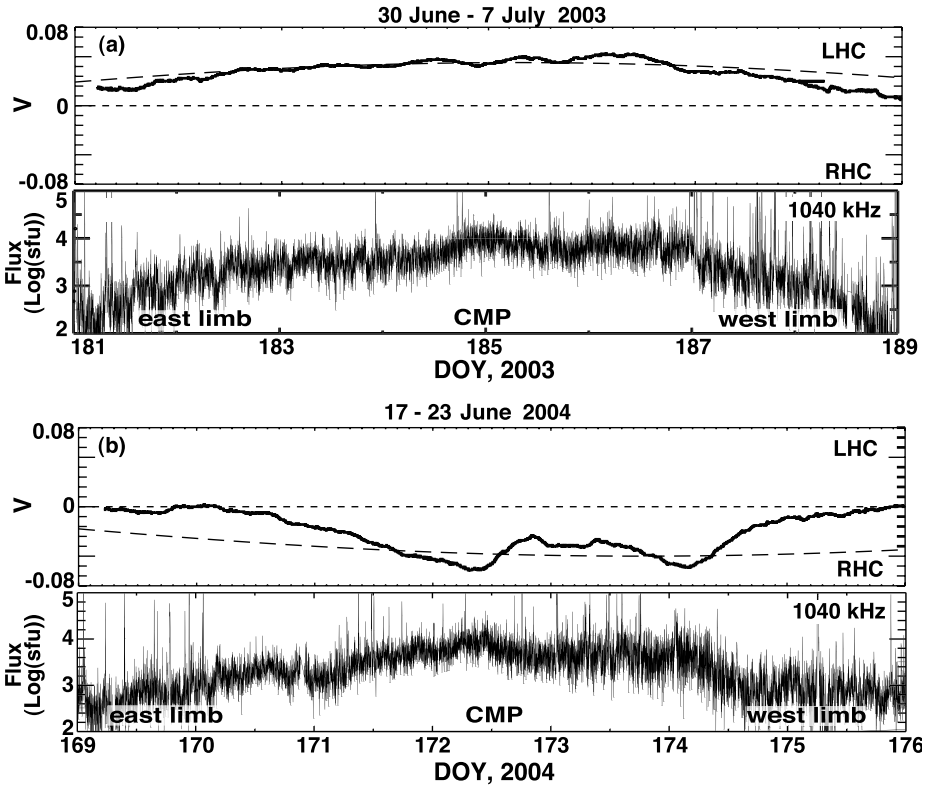

Figure 6 Center-to-limb variation of the circular polarization. (a) Results for the flux density and degree of circular polarization for the type III storm observed from 30 June to 7 July 2003. (b) Results for the flux density and degree of circular polarization for the type III storm observed from 17 to 24 June 2004.

and c indicate that the radio source at this frequency was near central meridian and slightly above the ecliptic plane. Figure 7d shows the source angular radius of about 5°.

Although there is nothing unusual about these derived spatial source parameters, what stands out for this storm is the unusually high degree of circular polarization that is evident in Figure 7e. The average degree of circular polarization at 1040 kHz on 8 September was $V = -0.0915 \pm 0.0013$, *i.e.*, nearly 10% RHC. The average degree of circular polarization for other days was somewhat smaller; $V = -0.0856 \pm 0.00120$ on 7 September and $V = -0.0749 \pm 0.00128$ on 9 September. The average circular polarization of the galactic component on 15 September was $V = 0.0015 \pm 0.0012$, again consistent with no circular polarization from this source.

As for other storms, the degree of circular polarization decreased systematically with frequency. Figure 8 displays the mean values for the degree of circular polarization from 148 to 1040 kHz. Although there may be some significant systematic deviations from a straight-line fit, the falloff of the degree of circular polarization is nevertheless approximately linear. The best straight-line fit to all the frequency values gives $|V| = -0.198 + 0.0411 \ln(f)$.

Although the morphological and spatial characteristics of this September storm do not differ in any significant way from other type III storms observed during solar cycle 23, it is notable for its unusually high value for the degree of circular polarization. We have found

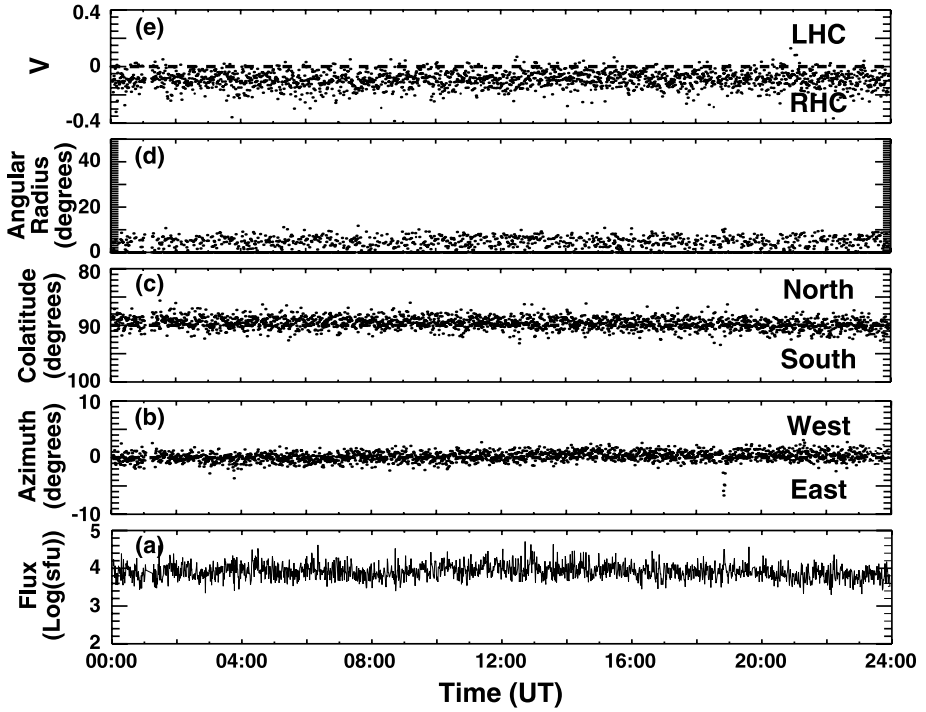

Figure 7 Results of the direction-finding/polarization analysis at 1040 kHz from 0 to 24 UT on 8 September 2004. (a) Radio source flux density as a function of time. (b) Radio source azimuth, relative to the *Wind* – Sun line. (c) Radio source colatitude, relative to the direction of the ecliptic plane. (d) Source angular radius. (e) Degree of circular polarization.

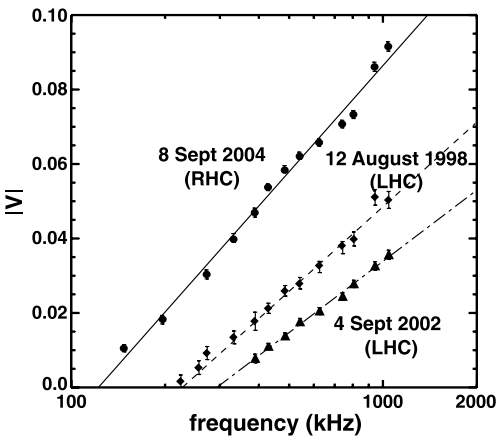

Figure 8 Mean values of the Stokes parameter $|V|$ deduced from the results of the direction-finding/polarization analysis for type III radio storms observed from 0 to 24 UT on 8 September 2004 (dots), on 12 August 1998 (diamonds), and on 4 September 2002 (triangles). The error bars correspond to the error in the mean. The sense of the polarization for each storm is also indicated.

no other type III storm with a degree of circular polarization significantly higher than 5%. In that sense this type III storm was unique.

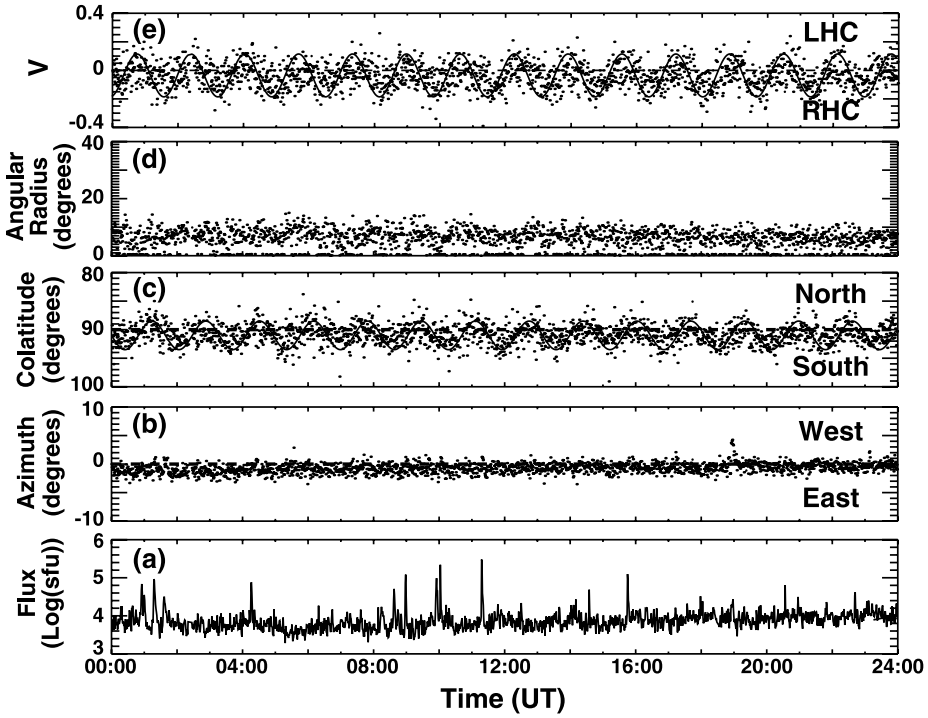

Figure 9 Results of the direction-finding/polarization analysis at 1040 kHz from 0 to 24 UT on 28 April 2000. (a) Radio source flux density as a function of time. (b) Radio source azimuth, relative to the *Wind* – Sun line. (c) Radio source colatitude, relative to the direction of the ecliptic plane. (d) Source angular radius. (e) Degree of circular polarization. The sine curves on (c) and (e) correspond to a sinusoidal oscillation of period 1.645 hours.

3.4. Interplanetary Type III Storm in April of 2000

This type III radio storm commenced on about 23 April and lasted until about 2 May 2000. Its central meridian crossing on 28 April suggests a possible association with either NOAA 8971 in the northern hemisphere or NOAA 8970 in the southern hemisphere. However, a type I noise storm observed in the northern hemisphere suggests that this type III storm was most likely associated with NOAA 8971.

The derived radio source parameters on 28 April 2000 with galactic background subtracted, are shown in Figure 9. The lower panel shows that the flux density of this storm was similar to that of the previous storms; the average flux density at 1040 kHz was about $10^{3.9}$ sfu or 9 dB above the level of the galactic background. Figures 9b and c indicate that the radio source at this frequency was approaching central meridian, a few degrees below the ecliptic plane. Figure 9d shows the source angular radius to be less than 10°.

Figure 9e shows that while the average degree of circular polarization was about 4% RHC, it exhibited a clear oscillatory behavior. A similar oscillatory behavior also appeared in the colatitudinal angle in Figure 9c. A power spectral analysis of the Stokes parameter V, shown in Figure 10, shows a clear peak at a frequency corresponding to 1.645 hours. In Figures 9c and e, we have superposed a sine wave with this period to make the oscillation pattern in these parameters more conspicuous. The oscillations of the colatitude are about

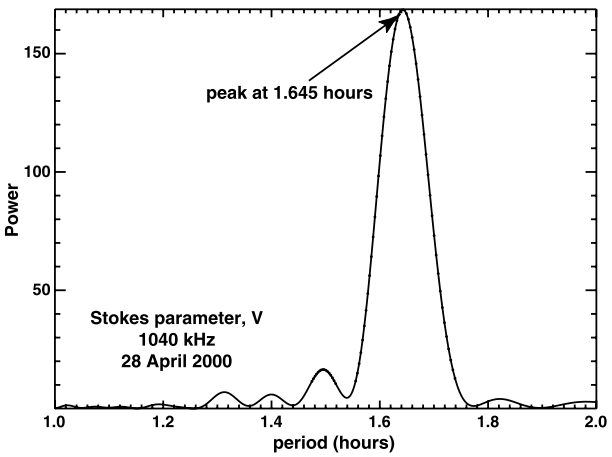

Figure 10 Spectral power of the Stokes parameter V at 1040 kHz as a function of period (in hours), showing the spectral peak at 1.645 hours.

80° out of phase with that of the circular polarization, but they appear to have the same period. The oscillatory behavior in the source parameters continued for essentially the entire duration of this type III storm, and was also present in these parameters derived at other observing frequencies, from about 500 kHz.

This is the only type III radio storm, observed during solar cycle 23, for which such an oscillatory behavior in the derived source parameters was clearly observed. It may represent a oscillatory mode of the associated quasi-stable helmet streamer in the active region from which this storm originated. However, we did not note anything unusual occurring on the Sun during this time period. We also do not know why this oscillation period does not appear in the flux density and/or in the azimuthal angle.

4. Discussion and Implications for the Solar Magnetic Field

4.1. Circular Polarization in Interplanetary Type III Storms

The polarization observed for the interplanetary type III storms was found to be RHC for some storms and LHC for others. We list in Table 1 the polarization characteristics of a representative sample of ten type III storms observed during solar cycle 23. The degree and sense of the circular polarization at 1 MHz is given in column 3. With one exception, all of the hectometric – kilometric type III radio storms, observed during solar cycle 23, exhibited degrees of circular polarization of about 5% or less at 1 MHz, which is independent of the average storm flux density, given in column 2.

It is of interest to investigate the relationship between the sense of the storm polarization and the polarity of the leading spot of the associated active region. As indicated above, there are usually a number of active regions on the Sun during the time of any given interplanetary type III storm. However, comparison of the central meridian crossing of the solar active regions with that of the storm radio sources, derived from the directional analysis, significantly narrows the possibilities. Due to the fact that the radio sources lie along the Archimedean spiral field lines emanating from the associated active region, the type III storm radio sources typically cross central meridian slightly later than the associated active region (Bougeret, Fainberg, and Stone, 1984b). Furthermore, as we have seen, it often happens that there are

Table 1 Interplanetary type III radio storm parameters and associated solar active regions.

Storm date (DD MM YYYY)	Flux log(sfu)	Max. pol. (%) at 1 MHz	Associated NOAA active region(s)	Polarity of the leading spot[1]
12 August 1998	4.0	+5.0 (LHC)	8297, 8299 (north)	+
23 March 2000	3.5	+5.0 (LHC)	8916, 8927 (north)	+
28 April 2000	3.9	−3.9 (RHC)	8971 (north)	+
13 July 2000	3.5	+3.0 (LHC)	9077 (north)	+
24 May 2001	3.9	+3.3 (LHC)	9463 (north)	+
04 September 2002	3.9	+3.6 (LHC)	10095, 10097 (north)	+
20 September 2002	3.7	−5.3 (RHC)	10123, 10119 (south)	−
05 July 2003	3.9	+4.8 (LHC)	10397 (north)	+
20 June 2004	3.8	−4.8 (RHC)	10635 (south)	−
08 September 2004	3.9	−9.2 (RHC)	10669, 10667 (south)	−

[1] '+' refers to fields out of the Sun; '−' to fields into the Sun.

two active regions, one north, the other south of the solar equator, at the expected solar longitude of the storm-associated active region. To distinguish which of these active regions is the origin of the type III storm, we have used the fact that the interplanetary type III storms, like their metric counterparts, are normally associated with metric type I noise storms. For each of the interplanetary storms analyzed, we therefore noted the location of the associated type I noise storm in the Nançay radioheliograph images (http://bass2000.obspm.fr/home.php). This usually allowed us to identify the hemisphere of the associated active region. The likely active regions, determined in this way, for the storms listed in Table 1, are given in the fourth column. We next used the ground-based (Solar Geophysical Data) and space-based (SOHO/MDI) (http://sohowww.nascom.nasa.gov/data/soho_images_form.html) solar magnetograms to determine the polarity of the leading spot of the storm-associated active region. These results are presented in column five in Table 1.

Comparison of columns 3 and 5 in Table 1 indicates a simple relationship between the sense of the polarization of the type III radio storm and the polarity of the leading sunspot, which is also the polarity of the associated solar hemisphere. With the exceptional case of the April 2000 storm, the polarity of the leading spot was the same as the sense of the wave polarization of the radio storm; a positive polarity of the leading spot corresponded to LHC radiation from the associated type III storm, and *vice versa*.

It is well known that the polarization of metric type I noise storms generally corresponds to the magnetic polarity of the dominant or leading sunspot (Stewart, 1985), with LHC (RHC) polarization corresponding to positive (negative) polarity of the leading spot. It has also been shown that the metric type III storms always have the same sense of polarization as that of the accompanying type I storm (Dulk, Suzuki, and Sheridan, 1984). The fact that we have found the polarization characteristics of the hectometric – kilometric type III storms to agree with those of the leading spot, and therefore, by implication, agree with the polarization of the type I and associated metric type III storms, further supports the suggestion that the interplanetary type III storms represent the low-frequency extensions of metric type III storms (Dulk, Suzuki, and Sheridan, 1984; Kai, Melrose, and Suzuki, 1985). Indeed, we do often find the hectometric – kilometric type III storm emissions continuing up through the highest WAVES observing frequency of 14 MHz and to 60 or 70 MHz, when

detected by the Green Bank Solar Radio Burst Spectrometer. It is therefore appropriate to compare the measured circular polarization observed in these two frequency regimes.

Metric type III radio storms are known to be circularly polarized, with degree of polarization up to about 25%. Unfortunately, we do not have polarization measurements for the metric type III storms that are the counterparts of the interplanetary storms considered in this paper, so no direct comparisons are possible. However, if we simply take the linear fits that we have obtained for the June 2004 and July 2003 storms in Figure 3 and extrapolate to the typical metric frequency of 100 MHz, we predict a degree of circular polarization between 15 and 25%, in agreement with what is typically measured for metric type III storms. This observation provides further confirmation that the metric and hectometric – kilometric type III storms do indeed represent the same physical phenomena. It also provides further confirmation that the circular polarization that we have measured below 1 MHz is intrinsic to the radio source, and is probably not significantly modified by the intervening plasma medium between the source and the observer (Zheleznyakov and Zlotnik, 1964).

While there is some observational evidence that the degree of circular polarization for individual type III bursts tends to increase with frequency at metric wavelengths (Mercier, 1990), we are not aware of any such results for metric type III storms. At hectometric – kilometric wavelengths, we have found that for many type III storms observed during solar cycle 23, the degree of circular polarization scales as the logarithm of the observing frequency. On Figure 8, we have also provided the measured degrees of circular polarization for two additional type III storms observed near central meridian passage, when the flux density and degree of polarization were maximum. The frequency dependence of the degree of polarization for the storm observed on 12 August 1998 is nearly identical to that of the 5 July 2003 storm shown in Figure 3; at 1 MHz it is $\approx$5% LHC and the slope of the best-fit straight line is also similar. We also show in Figure 8 the frequency dependence of the degree of circular polarization for a storm on 4 September 2002. Although this storm had a maximum degree of polarization at 1 MHz of only $\approx$3.6% LHC, it also exhibited an approximately linear dependence on the logarithm of frequency. This frequency variation of the degree of circular polarization, shown in Figures 3 and 8, is characteristic of interplanetary type III storms observed throughout solar cycle 23, from 1998 to 2005. We are not aware of any fundamental reason for the dependence of the observed polarization on the logarithm of the frequency; it is an empirical result.

We found that for many type III storms there was a clear center-to-limb variation in the degree of circular polarization, such as shown in Figure 6a. This center-to-limb variation is expected on the basis of the theory of type III bursts. Melrose, Dulk, and Smerd (1978) have shown that the degree of circular polarization for type III bursts should be proportional to the ratio of the electron cyclotron frequency to the plasma frequency. Since the calculated proportionality factor depends on the viewing angle relative to the magnetic field direction, a center-to-limb variation is expected.

In some storms we observed clear short-term variations in the degree of circular polarization, superposed on the center-to-limb variation. Although there are often short-term fluctuations in the flux densities ($\approx$hours), such as for the two storms shown in Figure 6, the fluctuations in the degree of circular polarization generally do not correlate with them. In Figure 6b, we show the average variation of the degree of circular polarization for the June 2004 type III storm, which is not well fitted by a simple $\cos\beta$ function. We believe that such short-term variations in the observed polarization are real and reflect physical changes in the plasma density or, more likely, in the magnitude of the magnetic field above active regions. Short-term variations in the degree of circular polarization are also commonly observed just prior to major coronal eruptions involving CMEs; this will be investigated in a forthcoming paper.

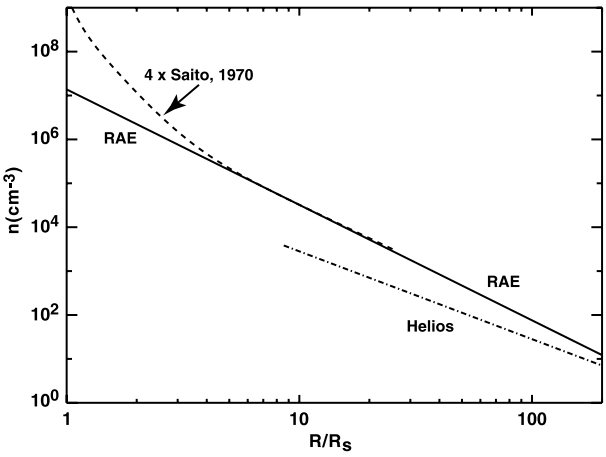

Figure 11 Coronal and interplanetary density profiles deduced from several different models.

4.2. Relationship to the Solar Magnetic Fields

According to the theory of type III emissions, the observed degree of circular polarization should be proportional to the ratio of the electron cyclotron frequency f_c to the plasma frequency f_p, *i.e.*,

$$|V| \propto a f_c / f_p, \tag{1}$$

where a is a complex factor that depends, among other things, on the viewing angle relative to the magnetic field direction (Melrose and Sy, 1972; Melrose, Dulk, and Smerd, 1978, 1980; Zlotnik, 1981; Melrose, 1985). The actual value of a is not well known. For the analyses below, we assume that $a \approx 0.2$ (Zlotnik, 1981). Once the plasma frequency profile is fixed by choosing an appropriate coronal density profile, our measurements of the type III storm polarization can therefore be used to deduce the magnitude and radial and temporal variations of the solar magnetic field above the solar active regions, from which these type III storm radio sources originate.

Analysis of type III radio storms has provided a coronal density profile that is appropriate above active regions; the so-called RAE density model, $n\ (\mathrm{cm}^{-3}) = 1.4 \times 10^7 (R/R_\odot)^{-2.63}$ (Fainberg and Stone, 1971). However, the RAE density profile was derived from type III radio sources observed only to a few MHz. It is therefore not expected to provide realistic densities in the low corona, below 10 $R_\odot$. For heliocentric distances less than 10 $R_\odot$, we therefore used the Saito (1970) coronal density model, multiplied by a factor of 4 to take into account the higher densities in the streamers that are the likely sites of the type III storm emissions. This latter model coincides with the RAE model at 10 $R_\odot$. These density profiles are shown by the solid and dashed curves in Figure 11. For comparison, we also show the Helios density model (dot-dashed curve) (Bougeret, King, and Schwenn, 1984c), which corresponds to the average in-situ solar wind densities measured by the Helios spacecraft.

Using the coronal density profile in Figure 11 and the circular polarization measurements given in Figure 3 for the July 2003 type III storm, Equation (1) gives the corresponding magnetic field profile shown by the solid curve in Figure 12. The magnetic field values derived from the actual polarization measurements are shown as the dots; the solid curve corresponds to the extrapolated solid line in Figure 3. The polarization observations for this interplanetary type III storm suggest a magnetic field magnitude of about 1/20 gauss

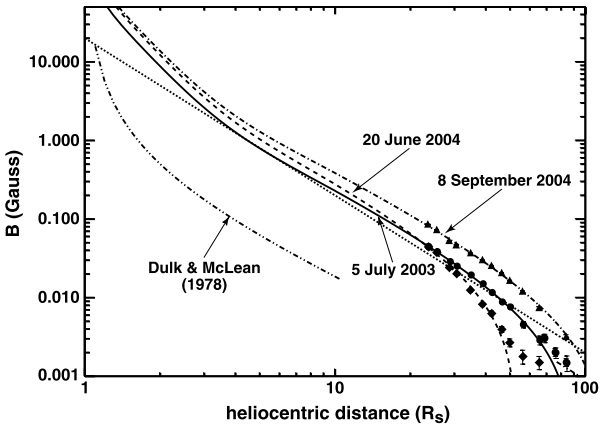

Figure 12 Magnitude of the coronal magnetic field deduced from the polarization measurements of type III radio storms: July 2003 storm (solid curve, dots); June 2004 storm (dashed curve, diamonds); September 2004 storm (dot-dashed curve, triangles). The magnitude of the magnetic field assuming a simple $1/R^2$ fall off is indicated by the dotted line. The Dulk and McLean (1978) magnetic field model is given by the double-dot-dashed curve.

at about 25 $R_\odot$, while the projected magnetic field magnitude at about 1.2 $R_\odot$ is about 50 gauss. Given that wide variations in the densities and magnetic fields are expected for different active regions, such values for the magnetic field magnitude are not inconsistent with those obtained from radio measurements made at higher frequencies, which correspond to heliocentric distances that are much closer to the solar surface (Mercier, 1990; Brosius and White, 2006).

While the actual values for the field magnitudes may be rather uncertain due to the uncertainty in the factor a in Equation (1), the comparison of the magnetic field radial and temporal variations, which depend only on the ratio, f_c/f_p, are likely still meaningful. The dashed and dot-dashed curves and superposed data points in Figure 12 show the derived magnetic field values for the June 2004 and September 2004 storms, respectively. Comparison of these derived coronal magnetic field strengths indicate that in the upper corona (>25 $R_\odot$) the magnetic field magnitude above the active region for the September 2004 storm was systematically higher, by about a factor of 2, than the field magnitudes above the active region associated with the July 2003 storm. On the other hand, the magnetic field above the active region for the June 2004 storm falls off with heliocentric distance much more rapidly than for the July 2003 storm.

A typical $1/R^2$ falloff of the coronal magnetic field is shown by the dotted line in Figure 12. In the region of our measurements, beyond 30 or 50 $R_\odot$, the derived field magnitudes all fall off more rapidly than $1/R^2$. Furthermore, in each case, the linear extrapolation of the storm polarization leads to a field strength in the lower corona that also increases more rapidly than would be expected for a field scaling as $1/R^2$. Thus, our measurements imply that the coronal magnetic field does not generally scale as $1/R^2$, at least above solar active regions. The reason is that the degree of polarization observed for these storm sources scales as $\ln(f)$, where f is the observing frequency. Equation (1) then implies that the magnitude of the magnetic field must scale as $f\ln(f)$. Since the density models imply that the observing (plasma) frequency scales with heliocentric distance approximately as $1/R$ (or $1/R^{1.3}$), the magnetic field will clearly not generally scale as $1/R^2$ in the corona. As is evident from Figure 12, the magnetic field tends to fall off significantly more rapidly both near the Sun and for heliocentric distances greater than about 30 to 50 $R_\odot$.

The magnetic field strengths above active regions are not well known and may vary considerable from one active region to another (Dulk and McLean, 1978). With this caveat in mind, Dulk and McLean (1978) have provided an empirical formula, $B(\text{gauss}) =$

$0.5[(R/R_\odot) - 1]^{-1.5}$, that qualitatively fits, to within a factor of three, a variety of observational estimates of the coronal magnetic fields above active regions. This model, which is expected to be valid for $R < 10\ R_\odot$, is shown in the double-dot-dashed curve in Figure 12. Except for an overall scaling factor, which may reflect the uncertainties in the factor, a, our extrapolated magnetic fields, based on the polarization measurements below 1 MHz, are qualitatively similar to this active region field model, both indicating that the magnetic field magnitude increases more rapidly than $1/R^2$ in the low corona.

It is well known that the magnitudes of the coronal magnetic fields that result from type III theory, through Equation (1), seem rather high as compared to some other determinations of these coronal fields (Dulk and McLean, 1978; Melrose, 1985). There can be a number of reasons for the discrepancy between our field values derived from Equation (1) and those obtained from the Dulk and McLean (1978) model. The linear extrapolation of the storm polarization may not be valid. However, this extrapolation gives reasonable values for the known circular polarization in metric type III storms. It is also possible that the value of the factor a may be in error. If the value of a were 2.0 instead of 0.2, our derived coronal fields would be very similar to those derived from the Dulk and McLean (1978) model. Alternatively, multiplying the Dulk and McLean (1978) model by a factor of 12 gives fields that are very similar to the values based on the polarization measurements. Finally, it may simply be that radio sources in active regions actually lie in regions of very large magnetic field strengths; large magnetic field strengths are typically deduced from radio observations, involving different radiation mechanisms (Mercier, 1990; Brosius and White, 2006). Thus, there may in fact be no compelling physical reason to reject these high magnitudes of the magnetic fields in solar active regions deduced from these radio observations.

Our observations also suggest that, as expected, the magnetic field profiles in the quasi-stable helmet streamer structures, from which the interplanetary storms originate, are stable in time. In Figure 3, we have also shown the polarization measurements on 2 July 2003 (open diamonds), which exhibit essentially the same falloff (slope) as on 5 July. We believe that this systematic downshift of the polarization values is due to the change in viewing angle of the storm radio sources between these two observation periods, and not due to actual changes in the magnitudes or radial dependence of the magnetic field structure above this active region structure. However, there are other cases, such as for the June 2004 storm shown in Figure 6b, where there are short-term variations in the degree of polarization, which may correspond to actual temporal changes in the magnetic field strengths and radial variation. This will be further explored in a future paper.

Since the ratio of the cyclotron to the plasma frequency is also directly related to the Alfvén speed, $v_A = 7.0 \times 10^3 f_c/f_p$, the Alfvén speed profile in the corona is directly obtained from these type III storm polarization measurements. The Alfvén speed profiles derived from the extrapolation of the measured polarization for the July 2003 and June 2004 type III storms are shown in Figure 13. These results indicate that the Alfvén speed rises rapidly and continuously in the low corona above these storm-associated active regions. The relatively large values of the Alfvén speed are of course a consequence of the relatively large values of the derived magnetic fields, shown in Figure 12.

The Alfvén speed profile is of current interest since it can provide important insights into the formation of coronal shocks and associated type II radio emissions in the corona (Mann *et al.*, 1999, 2003; Gopalswamy *et al.*, 2001). It is well known that if the magnetic field is assumed to fall off as $1/R^2$ in the corona, then, due to the fact that the density increases more rapidly than the field magnitude, the Alfvén speed profile will turn over in the low corona, as shown in dotted curve in Figure 13. However, as suggested by our observations, the magnetic

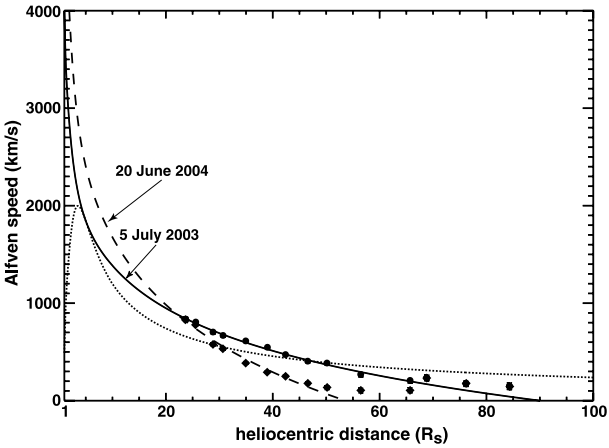

Figure 13 Alfvén speed profiles deduced from the magnetic field measurements for the June 2004 and July 2003 type III storms.

field above active regions does not scale as $1/R^2$. In our model calculations, based on the circular polarization observed for the type III storm radio sources, both the magnetic field and the density increase together in the low corona, so the resulting Alfvén speed continues to increase with decreasing heliocentric distances above the storm-associated active regions. This means that for a coronal disturbance propagating near an active region it is unlikely that a shock, which may produce type II radio emissions, will form above the active region. This suggests that the observed type II emissions in the low corona may generally originate outside the active region, where the Alfvén speed is lower and where a shock is more likely to form (Gopalswamy *et al.*, 2001).

5. Conclusion

In this paper, we presented a quantitative analysis of the circular polarization in interplanetary type III radio storms, observed during solar cycle 23. The measurements were made, below 1 MHz, by the WAVES experiment on the *Wind* spacecraft. We found that the degree of circular polarization, observed in all type III radio storms, was typically equal to or less than 5%. The sense of the polarization, for a given storm, was either right-hand or left-hand circular, but this polarization sense was maintained for the entire period of observation of a given storm. The sense of the storm polarization was found to be related to the polarity of the leading spot in the associated active region. Furthermore, we found that the degree of circular polarization for a given storm generally exhibited a center-to-limb variation and decreased systematically with decreasing frequency, scaling approximately as the logarithm of the frequency, for most storms that we have analyzed. We used these remote observations of the wave polarization to deduce the strengths and radial behaviors of the magnetic fields above solar active regions, finding that different storms imply different field strengths and radial dependences, which are generally stable for the entire observation period of the type III storm.

Acknowledgements The *Wind*/WAVES experiment is a collaboration of NASA/Goddard Space Flight Center, the Observatoire de Paris-Meudon and the University of Minnesota. M.J.R. acknowledges support, in part, from the NSF grant ATM-0417695.

References

Boishot, A., De la Noë, J., Møller-Pedersen, B.: 1970, *Astron. Astrophys.* **4**, 159.
Bougeret, J.-L., Fainberg, J., Stone, R.G.: 1983, *Science* **222**, 506.
Bougeret, J.-L., Fainberg, J., Stone, R.G.: 1984a, *Astron. Astrophys.* **136**, 255.
Bougeret, J.-L., Fainberg, J., Stone, R.G.: 1984b, *Astron. Astrophys.* **141**, 17.
Bougeret, J.-L., King, J.H., Schwenn, R.: 1984c, *Solar Phys.* **90**, 401.
Bougeret, J.-L., *et al.*: 1995, *Space Sci. Rev.* **71**, 231.
Brosius, J.W., White, S.M.: 2006, *Astrophys. J.* **641**, L69.
Cane, H.V., Stone, R.G., Fainberg, J., Steinberg, J.L., Hoang, S.: 1982, *Solar Phys.* **78**, 187.
Dulk, G.A., McLean, D.J.: 1978, *Solar Phys.* **57**, 279.
Dulk, G.A., Steinberg, J.L., Hoang, S.: 1984, *Astron. Astrophys.* **141**, 30.
Dulk, G.A., Suzuki, S., Sheridan, K.V.: 1984, *Astron. Astrophys.* **130**, 39.
Dulk, G.A., Steinberg, J.L., Lecacheux, A., Hoang, S., MacDowall, R.J.: 1985, *Astron. Astrophys.* **150**, L28.
Dulk, G.A., Steinberg, J.L., Hoang, S., Goldman, M.V.: 1987, *Astron. Astrophys.* **173**, 366.
Dulk, G.A., Leblanc, Y., Robinson, P.A., Bougeret, J.-L., Lin, R.P.: 1998, *J. Geophys. Res.* **103**, 17223.
Fainberg, J., Stone, R.G.: 1970a, *Solar Phys.* **15**, 222.
Fainberg, J., Stone, R.G.: 1970b, *Solar Phys.* **15**, 433.
Fainberg, J., Stone, R.G.: 1971, *Solar Phys.* **17**, 392.
Fainberg, J., Stone, R.G.: 1974, *Space Sci. Rev.* **16**, 145.
Ginzburg, V.I., Zheleznyakov, V.V.: 1958, *Sov. Astron.* **2**, 235.
Gopalswamy, N., *et al.*: 2001, *J. Geophys. Res.* **106**, 25261.
Gurnett, D.A.: 1975, *J. Geophys. Res.* **80**, 2751.
Hartz, T.R.: 1969, *Planet. Space Sci.* **17**, 267.
Kai, K., Melrose, D.B., Suzuki, S.: 1985, In: McLean, D.J., Labrum, N.R. (eds.) *Solar Radiophysics Studies of Emission from the Sun at Metre Wavelengths*, Cambridge University Press, New York, p. 415.
Kaiser, M.L.: 2003, *Adv. Space Res.* **32**, 461.
Kayser, S.E., Bougeret, J.-L., Fainberg, J., Stone, R.G.: 1987, *Solar Phys.* **109**, 107.
Kellogg, P.J.: 1980, *Astrophys. J.* **236**, 696.
Kellogg, P.J.: 1986, *Astron. Astrophys.* **169**, 329.
Kraus, J.D.: 1986, *Radio Astronomy*, Cygnus-Quasar Books, Powell, p. 4
Leblanc, Y., Dulk, G.A., Hoang, S., Bougeret, J.-L., Robinson, P.A.: 1996, *Astron. Astrophys.* **316**, 406.
Lecacheux, A., Steinberg, J.L., Hoang, S., Dulk, G.A.: 1989, *Astron. Astrophys.* **217**, 237.
Malitson, H.H., Fainberg, J., Stone, R.G.: 1973, *Astrophys. J.* **183**, L35.
Mann, G., Aurass, H., Klassen, A., Estel, C., Thompson, B.J.: 1999, In: *Proc. 8th SOHO Workshop, ESA SP-446*, 477.
Mann, G., Klassen, A., Aurass, H., Classen, H.T.: 2003, *Astron. Astrophys.* **400**, 329.
Manning, R., Fainberg, J.: 1980, *Space Sci. Instrum.* **5**, 161.
Melrose, D.B.: 1985, In: McLean, D.J., Labrum, N.R. (eds.) *Solar Radiophysics Studies of Emission from the Sun at Metre Wavelengths*, Cambridge University Press, New York, p. 177.
Melrose, D.B., Sy, W.N.: 1972, *Aust. J. Phys.* **25**, 387.
Melrose, D.B., Dulk, G.A., Gary, D.E.: 1980, *Proc. Astron. Soc. Aust.* **4**, 50.
Melrose, D.B., Dulk, G.A., Smerd, S.F.: 1978, *Astron. Astrophys.* **66**, 315.
Mercier, C.: 1990, *Solar Phys.* **130**, 119.
Parker, E.N.: 1958, *Astrophys. J.* **128**, 664.
Potter, D.W., Lin, R.P., Anderson, K.A.: 1980, *Astrophys. J.* **236**, L97.
Reiner, M.J.: 2001, *Space Sci. Rev.* **97**, 129.
Reiner, M.J., Kaiser, M.L.: 1999, *Geophys. Res. Lett.* **26**, 397.
Reiner, M.J., Stone, R.G.: 1986, *Solar Phys.* **106**, 397.
Reiner, M.J., Stone, R.G.: 1989, *Astron. Astrophys.* **217**, 251.
Reiner, M.J., Stone, R.G.: 1990, *Solar Phys.* **125**, 371.
Reiner, M.J., Fainberg, J., Stone, R.G.: 1995, *Science* **270**, 461.
Reiner, M.J., Stone, R.G., Fainberg, J.: 1992, *Astrophys. J.* **394**, 340.
Reiner, M.J., Fainberg, J., Kaiser, M.L., Stone, R.G.: 1998, *J. Geophys. Res.* **103**, 1923.
Reiner, M.J., Kaiser, M.L., Karlický, M., Jiřička, K., Bougeret, J.-L.: 2001, *Solar Phys.* **204**, 123.
Robinson, P.A.: 1992, *Solar Phys.* **139**, 147.
Robinson, P.A., Cairns, I.H., Gurnett, D.A.: 1993, *Astrophys. J.* **407**, 790.
Saito, K.: 1970, *Ann. Tokyo Astron. Obs. Ser. 2* **12**, 53.
Sakurai, K.: 1971, *Solar Phys.* **16**, 125.
Steinberg, J.L., Hoang, S., Dulk, G.A.: 1985, *Astron. Astrophys.* **150**, 205.

Steinberg, J.L., Dulk, G.A., Hoang, S., Lecacheux, A., Aubier, M.G.: 1984, *Astron. Astrophys.* **140**, 39.
Stewart, R.T.: 1985, *Solar Phys.* **96**, 381.
Stewart, R.T., Labrum, N.R.: 1972, *Solar Phys.* **27**, 192.
Wright, C.S.: 1980, *Proc. Astron. Soc. Aust.* **4**, 62.
Zheleznyakov, V.V., Zlotnik, E.Y.: 1964, *Sov. Astron.* **7**, 485.
Zlotnik, E.Y.: 1981, *Astron. Astrophys.* **101**, 250.